Supporting Information for:

A Pyrrolyl-based Triazolophane: A Macrocyclic Receptor with CH and NH Donor Groups That Exhibits a Preference for Pyrophosphate Anions

Jonathan L. Sessler,*,[†] Jiajia Cai,[†] Han-Yuan Gong,[†] Xiaoping Yang,[†] Jonathan F. Arambula,[†] Benjamin P. Hay[‡]

Department of Chemistry & Biochemistry, 1 University Station-A5300, The University of Texas, Austin, Texas 78712-0165, and Chemical Sciences Division, Oak Ridge National Laboratory, Oak Ridge, Tennessee 37830-6119

Contents

Section S1: General Procedures, Details of Describing the Synthesis and Characterization of Compounds 4 and 1

General Procedures

All reagents and starting materials were obtained from commercial suppliers and used as received unless otherwise noted. Column chromatography was performed on silica gel (40-63 μm, Silicycle, Canada) and Alumina N (50-200 μm, Dynamic Adsorbents Inc., USA). Nuclear magnetic resonance (NMR) spectra were recorded on Varian Mercury 400, Varian Inova 500, and Varian DirectDrive 600 instruments. UV-vis spectra were recorded on a Cary 5000 UV-Vis-NIR Spectrophotometer. Low resolution ESI mass spectra were measured using either a Finnigan LCQ Quadrupole Ion Trap Mass Spectrometer or a Thermo LTQ-XL linear Ion Trap Mass Spectrometer. High resolution ESI mass spectra were obtained on an Ion Spec Fourier Transform mass spectrometer (9.4 T).

Synthetic Experimental

1,3-Bis(pyrro-2-yl)(1,4)-1,2,3-triazolobenzene, 4: A solution of the 3,5-diazido-1-*tert*-butylbenzene **2** (432.2 mg, 2.0 mmol), and 2-ethynylpyrrole-1-carboxylic acid *tert*-butyl ester **3** (840.8 mg, 4.4 mmol), sodium ascorbate (40.0 mg, 0.2 mmol), and $CuSO_4$ (5.0 mg, 0.02 mmol) in a mixture of 14 mL EtOH, 6 mL H_2O and 2 mL toluene was stirred at ambient temperature for 24 hrs. After removal of the solvents *in vacuo*, a brown solid was obtained. This solid was dissolved in CH_2Cl_2 and washed with water (3×30 mL). The aqueous phase was extracted twice with CH_2Cl_2 (2×50 mL). The organic extracts were combined and dried over $MgSO_4$ and then concentrated under reduced pressure. The brown solid obtained as a result was then dissolved in anhydrous THF and treated with 10 eqiv. sodium *tert*-butoxide and left to stir overnight. The volatiles were removed *in vacuo* and the brown solid obtained was washed with water (3×30 mL), extracted with ethyl acetate (2 × 50 mL), dried over $MgSO_4$ and concentrated under reduced pressure. The crude product was purified by column chromatography (alumina neutral, CH_2Cl_2: CH_3OH, 10:0.1, eluent) and recrystallized from THF and hexane to afford 188 mg (24%, 0.47 mmol) of **4** as a pale brown solid. ^{1}H NMR (DMSO-d_6, 400 MHz) [ppm], δ 11.52 (s, 2 H, NH), 9.11 (s, 2 H, -N-C**H**=C-), 8.35 (t, *J*=1.8 Hz, 1 H, CH), 8.03 (d, *J*=1.8 Hz, 2 H, CH), 6.87 (dd, J_1=4.0 Hz, J_2=2.4 Hz, 2 H, pyrrole-α-H), 6.51 (m, 2 H, pyrrole-β-H), 6.16 (dd, J_1=5.8 Hz, J_2=2.7 Hz, 2 H, pyrrole-β-H), 1.45 (s, 9 H, CH_3); ^{13}C-NMR (*d*-DMSO, 100 MHz) [ppm], δ 31.0, 35.6, 106.7, 109.0, 109.1, 116.8, 117.8, 119.5, 122.0, 137.7, 142.8, 155.4; MS (HR-ESI) Calcd. for $C_{22}H_{23}N_8$ ($M+H^+$) 399.2046; Found 399.2038 ($M+H^+$).

Calix[2]1,3-bis(pyrro-2-yl)(1,4)-1,2,3-triazolo-phane, 1: Compound **4** (500 mg, 1.256 mmol) in acetone (250 mL) was placed in a 1000 mL three-way round bottom flask and degassed for 30 min by bubbling with argon. While flushing the reaction vessel with argon, TFA (20 mL, 0.267 mol) was then added dropwise. The resulting solution was then stirred for 3 hours at ambient temperature before being quenched via the addition of solid NaOH (11 g, 0.275 mol). Evaporation of the reaction mixture afforded a brown

solid. To this crude product, dichloromethane (100 mL) and water (100 mL) were added. The organic phase was then separated off and washed three times with water (3×100 mL). The organic layer was dried over anhydrous $MgSO_4$ and evaporated *in vacuo* to yield a brown solid. This brown solid was purified by column chromatography (silica gel, CH_2Cl_2: CH_3OH, 10:0.1, eluent) and then followed by recrystallization from $CHCl_3$ and CH_3OH to give 54 mg (10%, 0.062 mmol) of **1** as a white solid. ^{1}H NMR ($CDCl_3$, 400 MHz) [ppm], δ 8.88 (s, 4 H, NH), 8.01 (s, 4 H, -N-C**H**=C-), 7.83 (d, *J*=2.4 Hz, 4 H, CH), 7.68 (t, *J*=2.0 Hz, 2 H, CH), 6.47 (m, 4 H, pyrrole-β-H), 6.21 (m, 4 H, pyrrole-β-H), 1.77 (s, 12 H, CH_3), 1.43 (s, 18 H, CH_3); ^{13}C-NMR ($CDCl_3$, 100 MHz) [ppm], δ 29.3, 31.4, 35.9, 36.0, 105.9, 107.3, 111.9, 116.9, 118.5, 121.4, 138.0, 140.6, 142.9, 156.2; MS (HR-ESI) Calcd. for $C_{50}H_{53}N_{16}$ ($M+H^+$) 877.4639; Found 877.4644 ($M+H^+$).

Spectroscopic data for: 1,3-bis(pyrro-2-yl)(1,4)-1,2,3-triazolobenzene (4) and calix[2]1,3-bis(pyrro-2-yl)(1,4)-1,2,3-triazolo-phane (1).

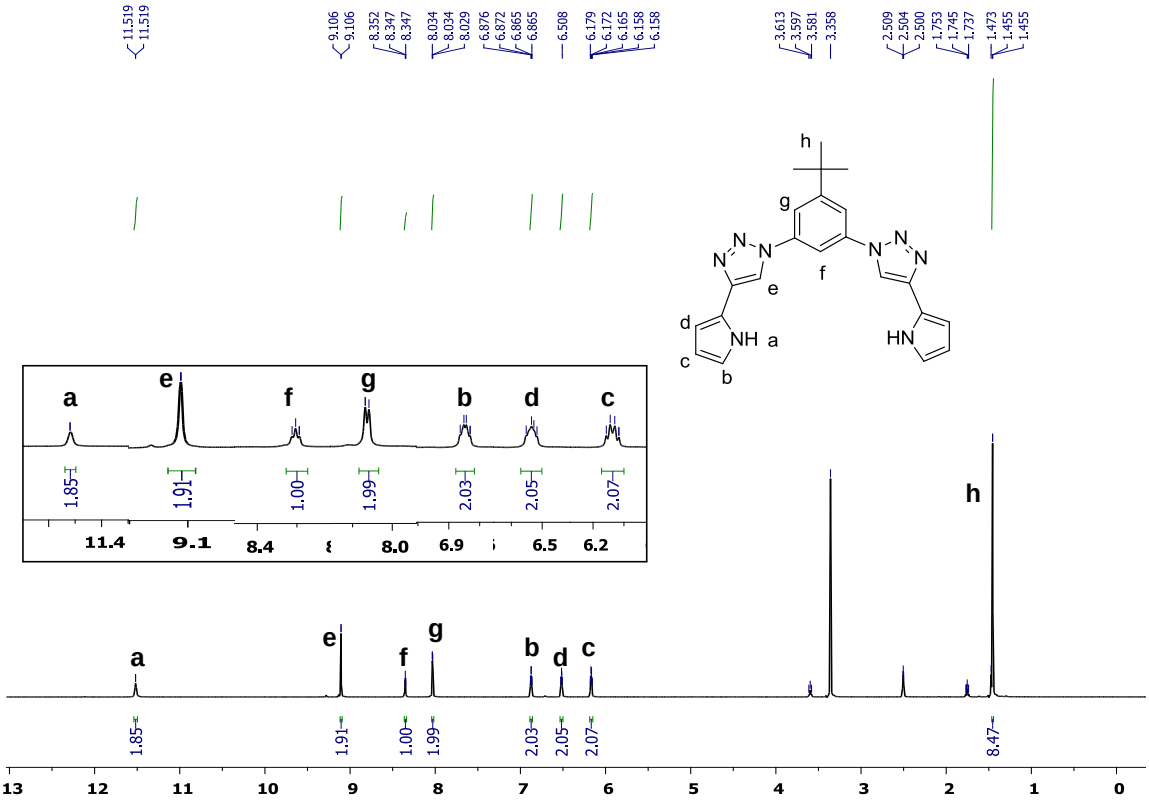

Figure S1: ^{1}H NMR spectrum of **4** recorded in DMSO-d_6 (the peaks at 3.59, 1.75 ppm belong to the solvent, THF) at 300 K.

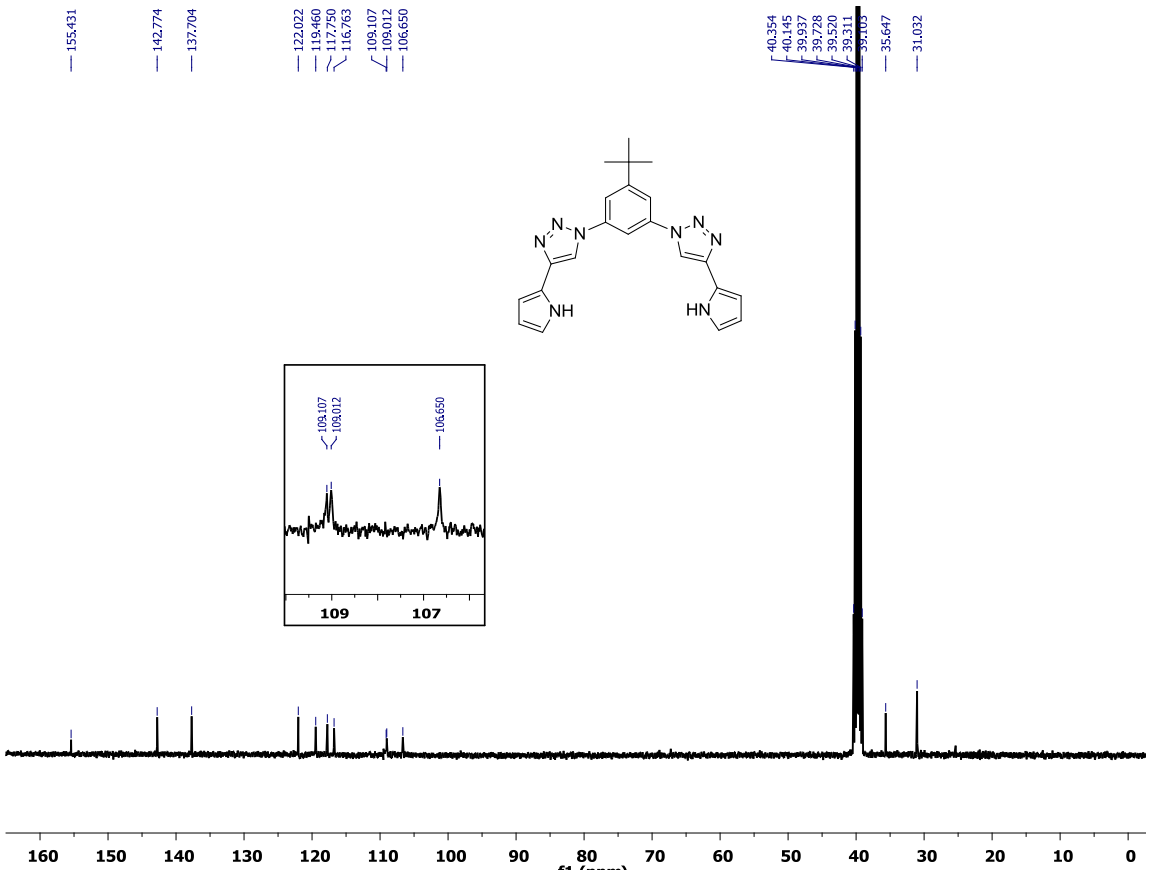

Figure S2: ^{13}C NMR spectrum of **4** recorded in DMSO-d_6 at 300 K.

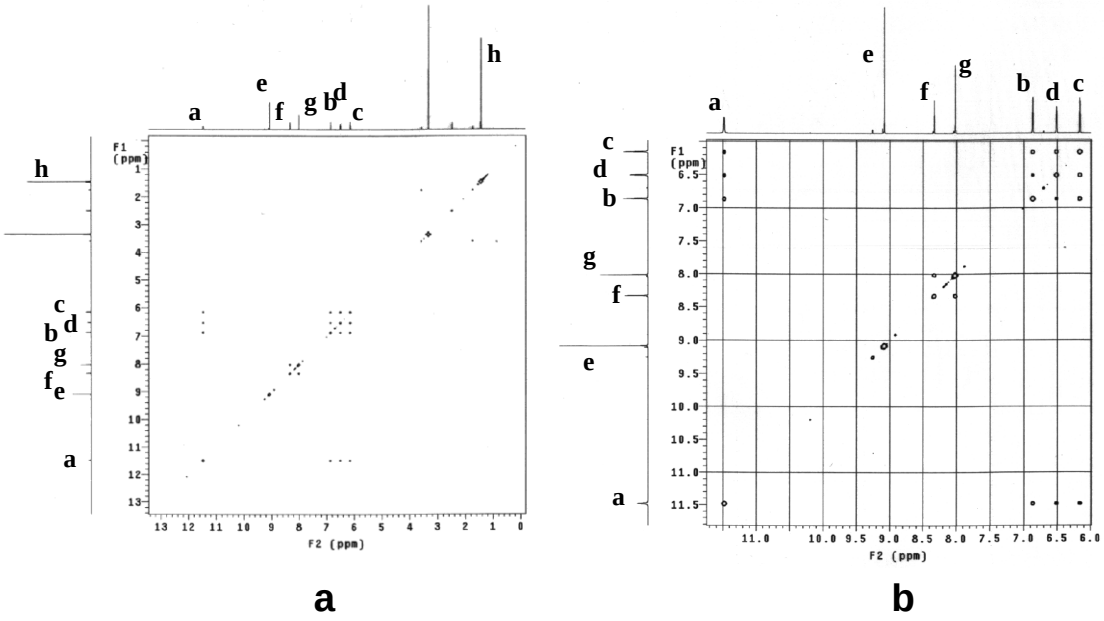

Figure S3: (a) Full view and (b) expanded view of the 2D COSY NMR spectrum of **4** recorded in DMSO-d_6 at 300 K.

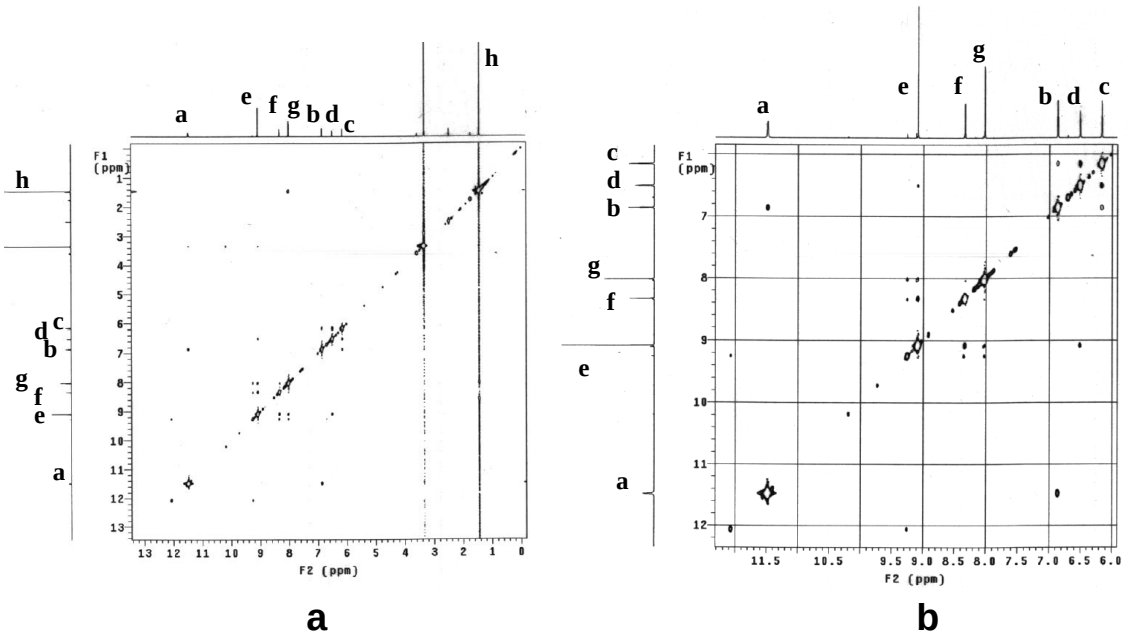

Figure S4: (a) Full view and (b) expanded view of the 2D NOESY NMR spectrum of **4** recorded in DMSO-d_6 at 300 K.

Note: The NOESY spectrum supports the following contentions:
1) The pyrrole α-protons (b) have corresponding signals with the pyrrole β-protons (c) and pyrrole NH (a).
2) The pyrrole β-H (d) have corresponding signals with the triazole CH (e) and pyrrole β-H (c) protons.
3) That the pyrrole β-H (c) have corresponding signals with both the pyrrole β-H (d) and pyrrole α-H (b) protons.

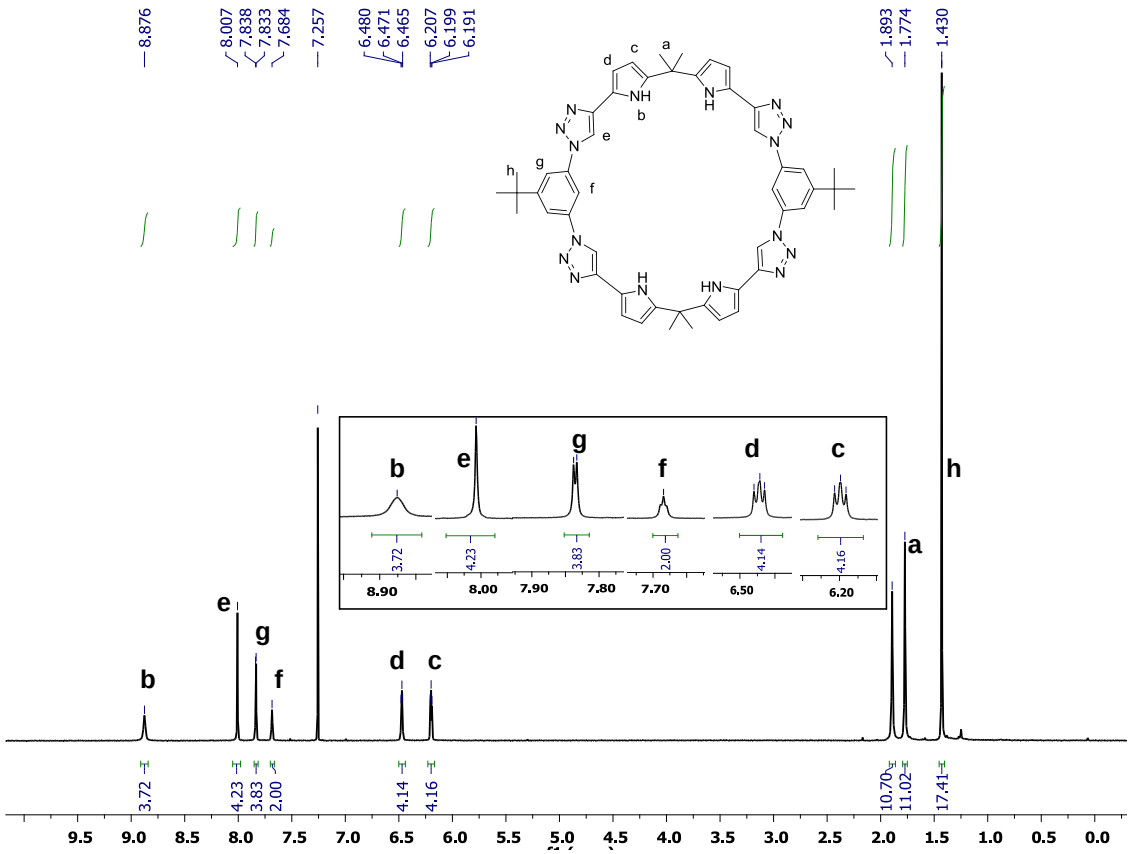

Figure S5: ^{1}H NMR spectrum of **1** recorded in $CDCl_3$ at 300 K. Note: The peak 1.89 ppm is ascribed to H_2O.

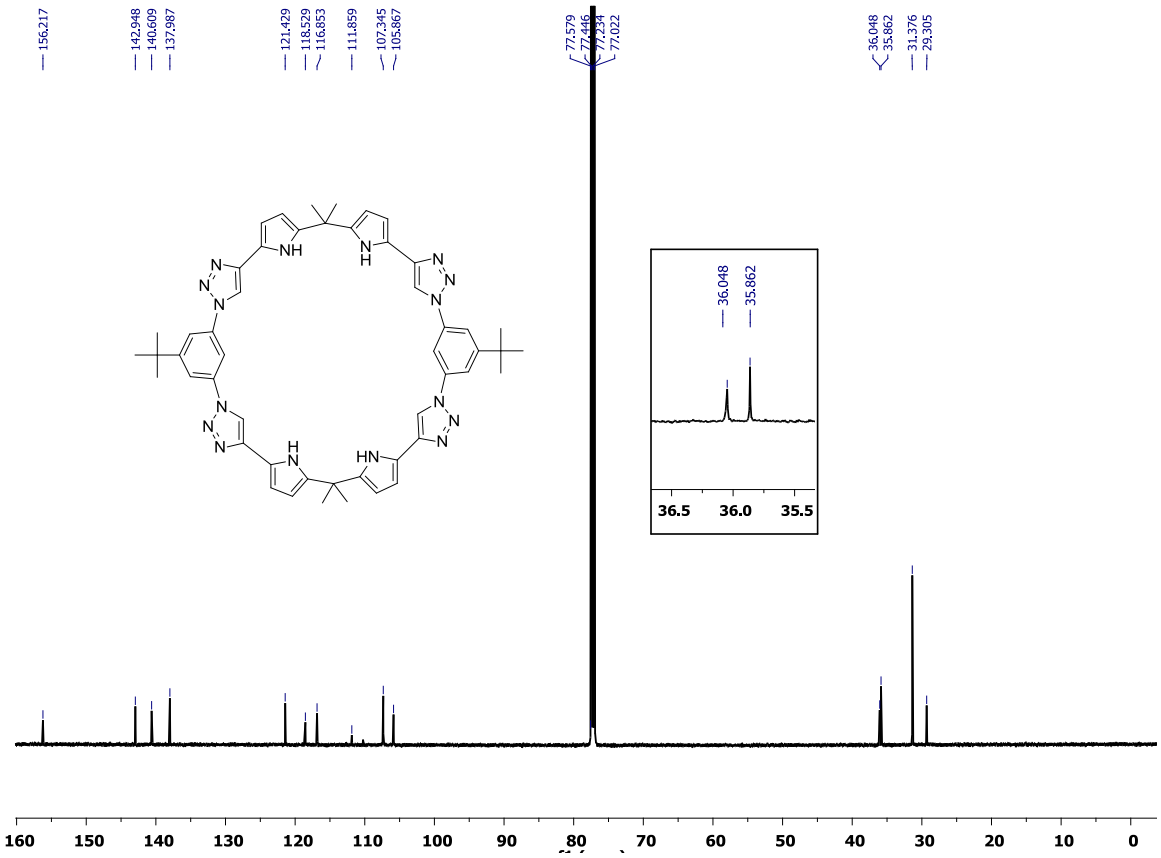

Figure S6: ^{13}C NMR spectrum of **1** recorded in $CDCl_3$ at 300 K.

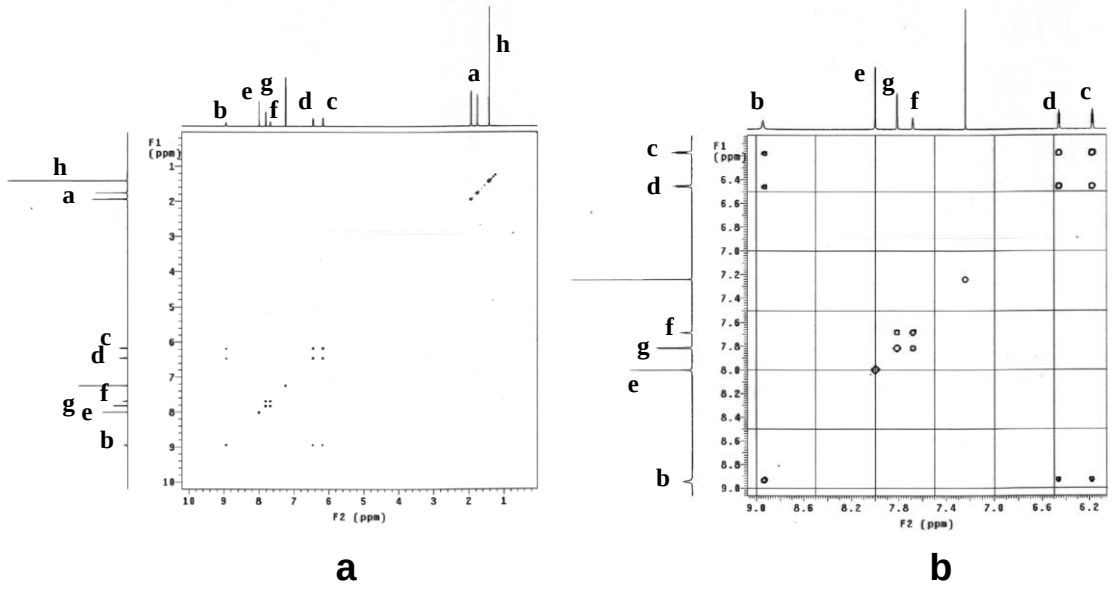

Figure S7: (a) Full view and (b) expanded view of the 2D COSY NMR spectrum of **1** recorded in $CDCl_3$ at 300 K.

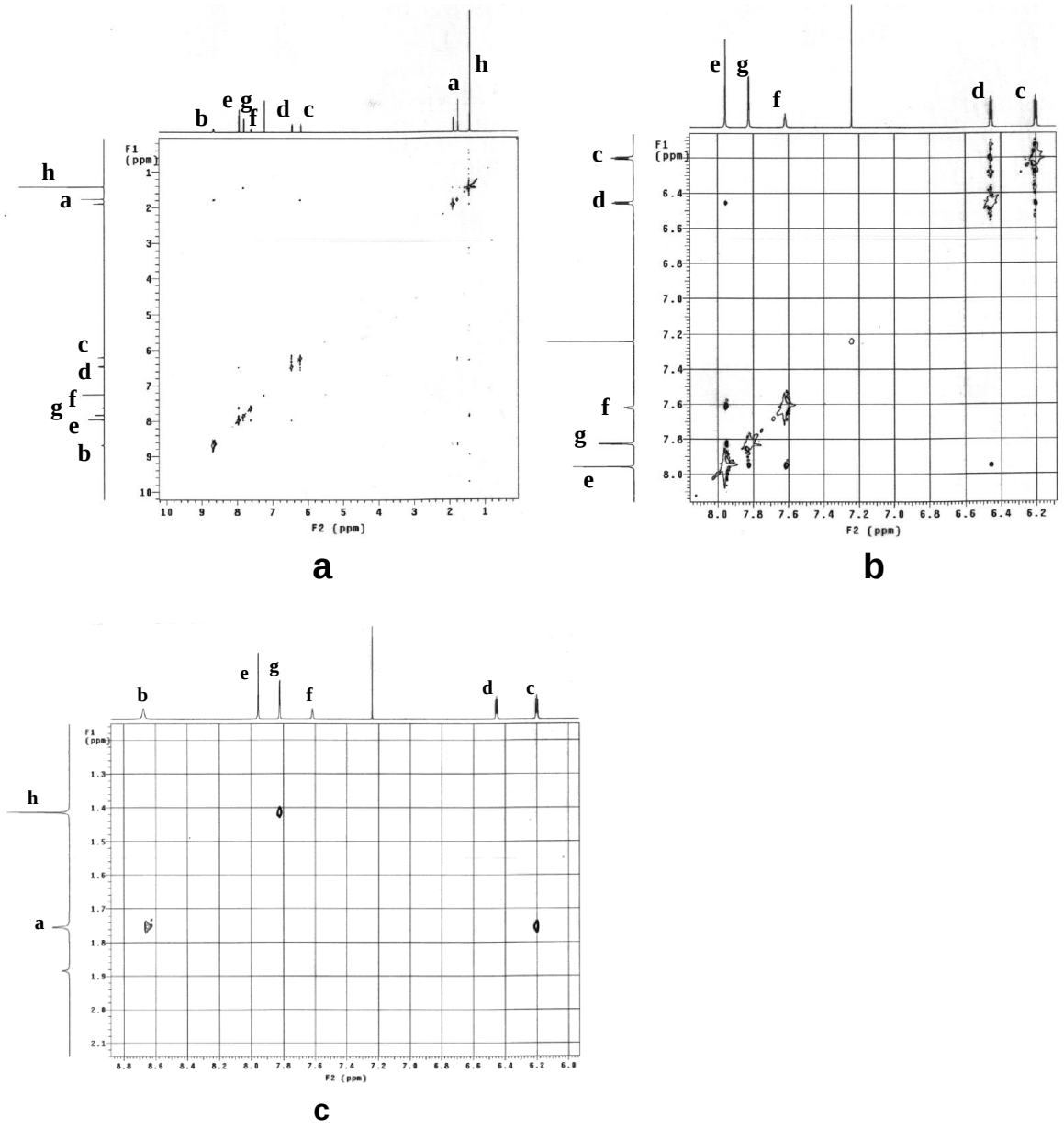

Figure S8: (a) Full view and (b), (c) expanded views of the 2D NOESY NMR spectrum of **1** recorded in $CDCl_3$ at 300 K.

Conformation analysis for macrocycle 1 in $CDCl_3$.

The ^1H NMR spectrum of **1** recorded in $CDCl_3$ at 300 K showed a set of high resolution signals, which is consistent with the macrocycle either having a fixed conformation with high symmetry or a flexible structure and being involved in a fast reversible equilibrium process (Figure S5).[1-4] The 2D NOESY NMR spectrum, Figure S8, provides evidence that the triazole CH proton (e) has signals that correspond with the protons on the benezene subunit (g), (f).

Taken in concert, these findings are not consistent with a fixed conformation (Figure S9a, b) or with the existence of a single non-equilibrating conformation (Figure S9c). Because only one set of signals is seen for hydrogen atoms e, g, f., we propose that the compound has a flexible conformation in solution; see main text.

To probe this hypothesis further, variable temperature ^1H NMR spectral studies were carried out (Figure S10). At ambient temperature, the NMR spectra gave defined peaks consistent with bond rotation faster than the NMR time scale. As the temperature was decreased, peak broadening became evident. As detailed in the text proper, we attribute this broadening to slowed rotation of the molecule, which allows for the detection of several different conformations.

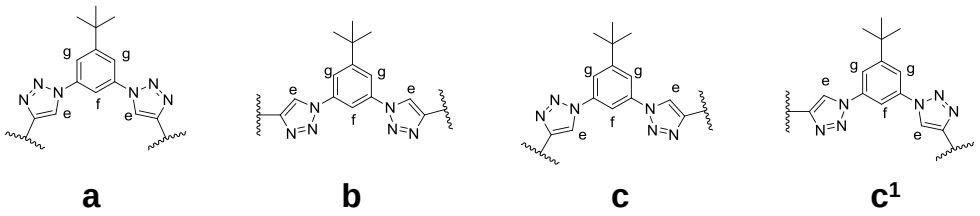

Figure S9: Limiting conformations for the fragments in **1** used to interpret the NOESY NMR spectra. Note that the conformers shown, c and c^1 are symmetry related.

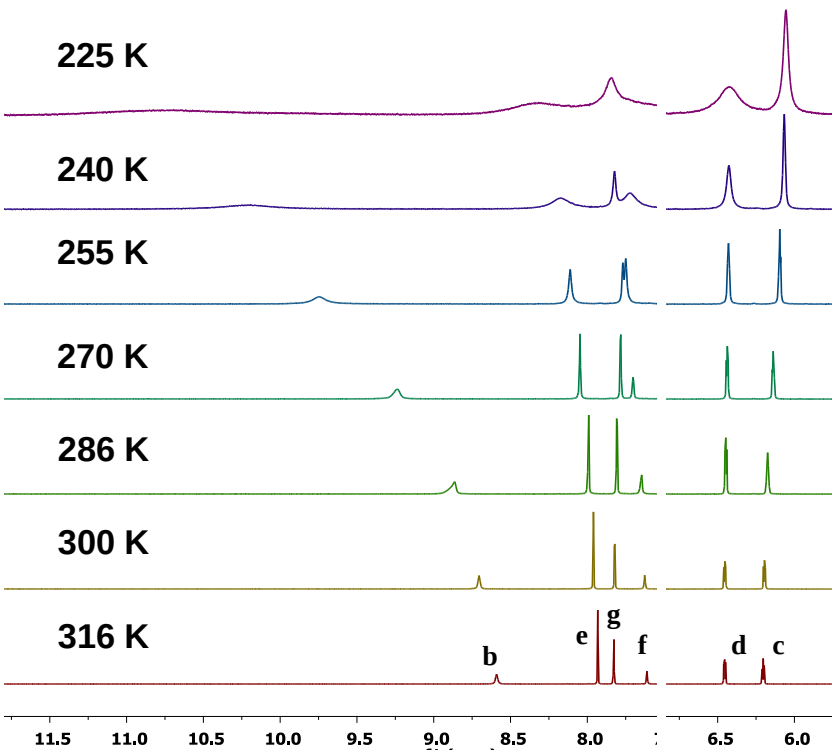

Figure S10: Variable temperature ^{1}H NMR spectrum of macrocycle **1** in $CDCl_3$.

Section S2: Details of Fitting UV-vis Binding Curves and NMR Spectroscopic Binding Studies

Anion Binding Studies

UV-Vis Anion Recognition Study:
Stock solutions of the host molecule being studied were made up in chloroform with the final concentrations being 1×10^{-5} M. Stock solutions of the guest in question were prepared by dissolving 100 - 300 equivalents of the tetrabutylammonium salts of the anions under study in 5 mL stock solutions of the host. Making up the anion source solutions in this way allowed the binding studies to be carried out without having to make mathematical corrections to account for changes in host concentration as the result of dilution effects.

The general procedure for the UV-Vis binding studies involved making sequential additions of titrant (anionic guest) using Hamilton pipettes to a 3 mL aliquot of the host stock solution in a spectrometric cell. The data was then collated and combined to produce plots that showed the changes in host spectral features as a function of guest concentration.

Job Plot Construction:
Stock solutions of the macrocycle (1.0×10^{-5} M) and $TBA_3HP_2O_7$ (1.0×10^{-5} M) were prepared separately in $CHCl_3$. For the other anions, stock solutions of the macrocycle (5.0×10^{-5} M) and the tetrabutylammonium anion salts (5.0×10^{-5} M) were prepared separately in $CHCl_3$. The UV-Vis spectrum was taken for each of 11 different solutions containing a total of 3.0 mL of the macrocycle **1** and tetrabutylammonium salt in the following ratios: 3.0:0, 2.7:0.3, 2.4:0.6, 2.1:0.9, 1.8:1.2, 1.5:1.5, 1.2:1.8, 0.9:2.1, 0.6:2.4, 0.3:2.7 and 0:3.0. Job's plots were constructed by plotting $A_{obs}–A_M–A_{anion}$ against the γ-coordinate. (γ = [host] / ([host] + [guest]))

Calculations of Equilibrium Constants, K_a
Upon addition of tetrabutylammonium salts, the UV spectra changed gradually. These changes were ascribed to anion binding, with the corresponding association constants (K_a) being determined by nonlinear curve fitting of the curves obtained by plotting the absorbance changes at a λ value where the spectral change was maximal (ΔA) against the concentration of the tetrabutylammonium anion salt added, $[X^-]$. The data was fitted to the equation,

$$\Delta A = A\cdot\{([\mathbf{1}] + [X^-] + (1/K_a)) – \{([\mathbf{1}] + [X^-] + (1/K_a))^2 – (4\cdot[\mathbf{1}]\cdot[X^-])\}^{1/2}\} / (2\cdot[\mathbf{1}])$$

where, the one unknown parameter is K_a, the value of the association constant; this value was obtained by the fit to the data with good fits (e.g., $R\hat{}2 \geq 0.99$) being obtained unless noted otherwise.

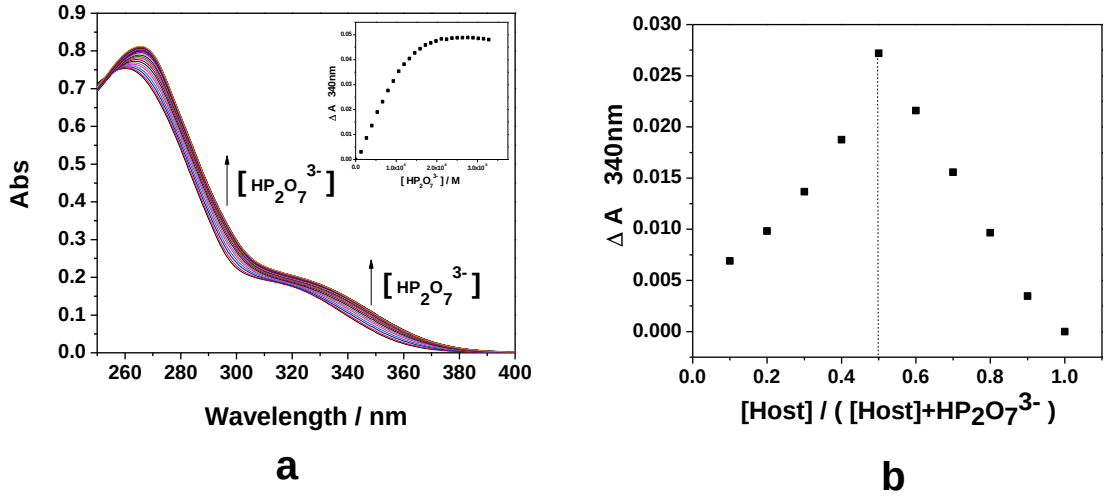

Figure S11. (a) UV-vis spectra of **1** (1.00×10^{-5} M) in chloroform with increasing ((*n*-Bu)$_4$N)$_3$HP$_2$O$_7$ (0 ~ 3.0×10^{-5} M). (b) Job plot for the interaction between host **1** and ((*n*-Bu)$_4$N)$_3$HP$_2$O$_7$ in chloroform with [host + guest] = 1.00×10^{-5} M. A maximum value at 0.5 is seen; this is consistent with a 1:1 (host: guest) binding stoichiometry.

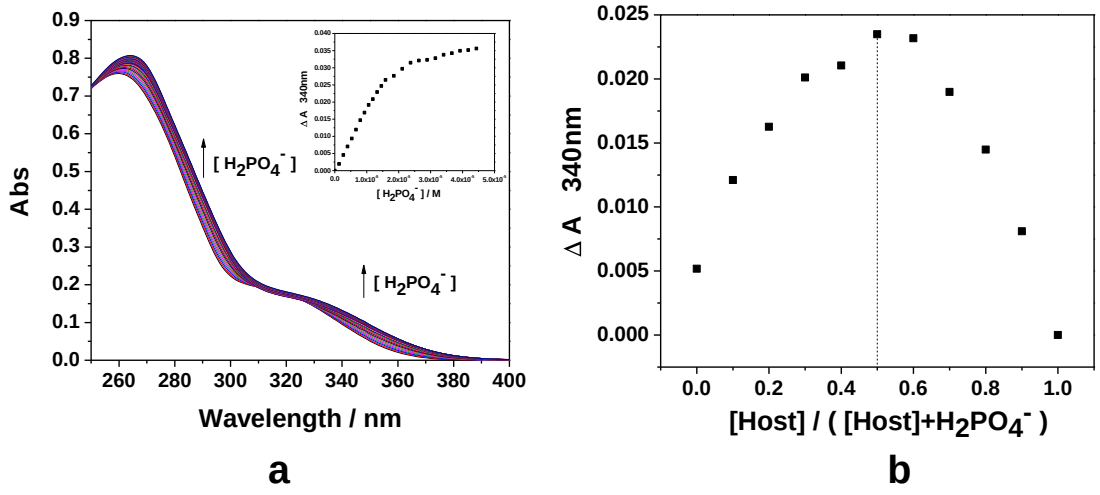

Figure S12. (a) UV-vis spectra of **1** (1.00×10^{-5} M) in chloroform with increasing (*n*-Bu)$_4$NH$_2$PO$_4$ (0 ~ 5.0×10^{-5} M). (b) Job plot for the interaction between host **1** and (*n*-Bu)$_4$NH$_2$PO$_4$ in chloroform with [host + guest] = 5.00×10^{-5} M. A maximum value at 0.5 is seen; this is consistent with a 1:1 (host: guest) binding stoichiometry.

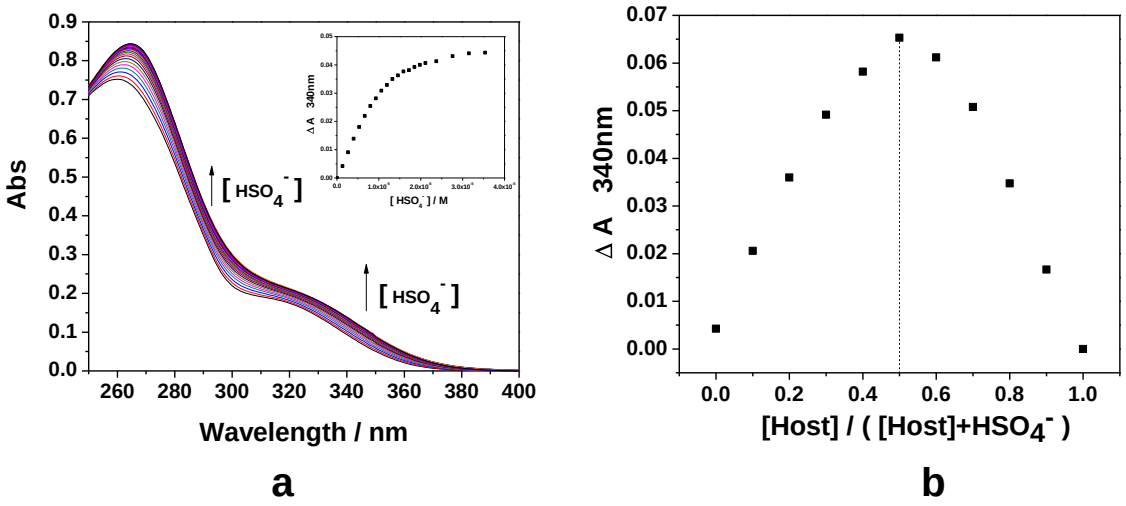

Figure S13. (a) UV-vis spectra of **1** (1.00×10^{-5} M) in chloroform with increasing (n-Bu)$_4$NHSO$_4$ (0 ~ 3.0×10^{-5} M). (b) Job plot for the interaction between host **1** and (n-Bu)$_4$NHSO$_4$ in chloroform with [host + guest] = 5.00×10^{-5} M. A maximum value at 0.5 is seen; this is consistent with a 1:1 (host: guest) binding stoichiometry.

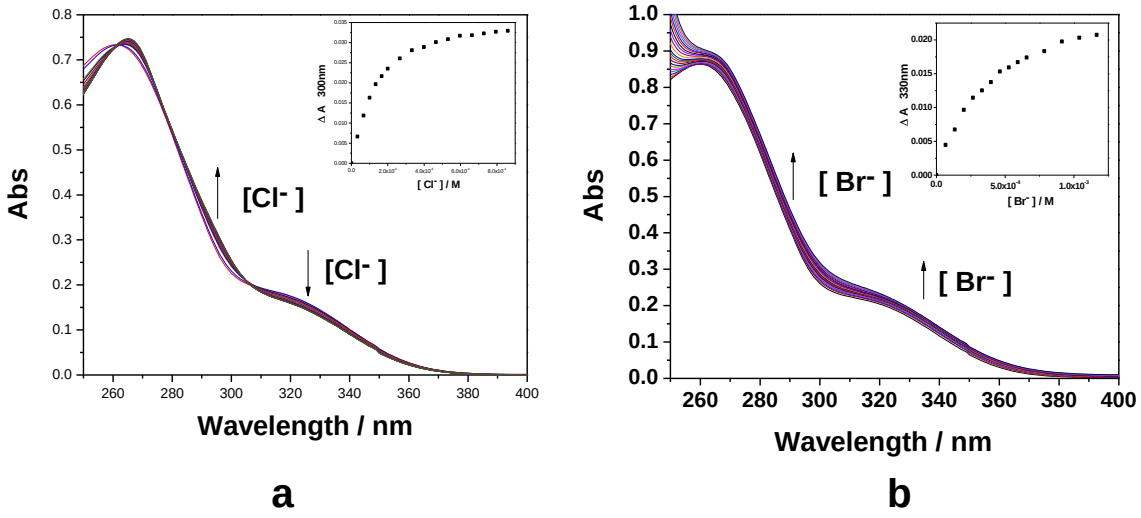

Figure S14. (a) UV-vis spectra of **1** (1.00×10^{-5} M) in chloroform with increasing (n-Bu)$_4$NCl (0 ~ 8.0×10^{-4} M). (b) UV-vis spectra of **1** (1.00×10^{-5} M) in chloroform with increasing (n-Bu)$_4$NBr (0 ~ 1.25×10^{-3} M).

Binding Isotherms

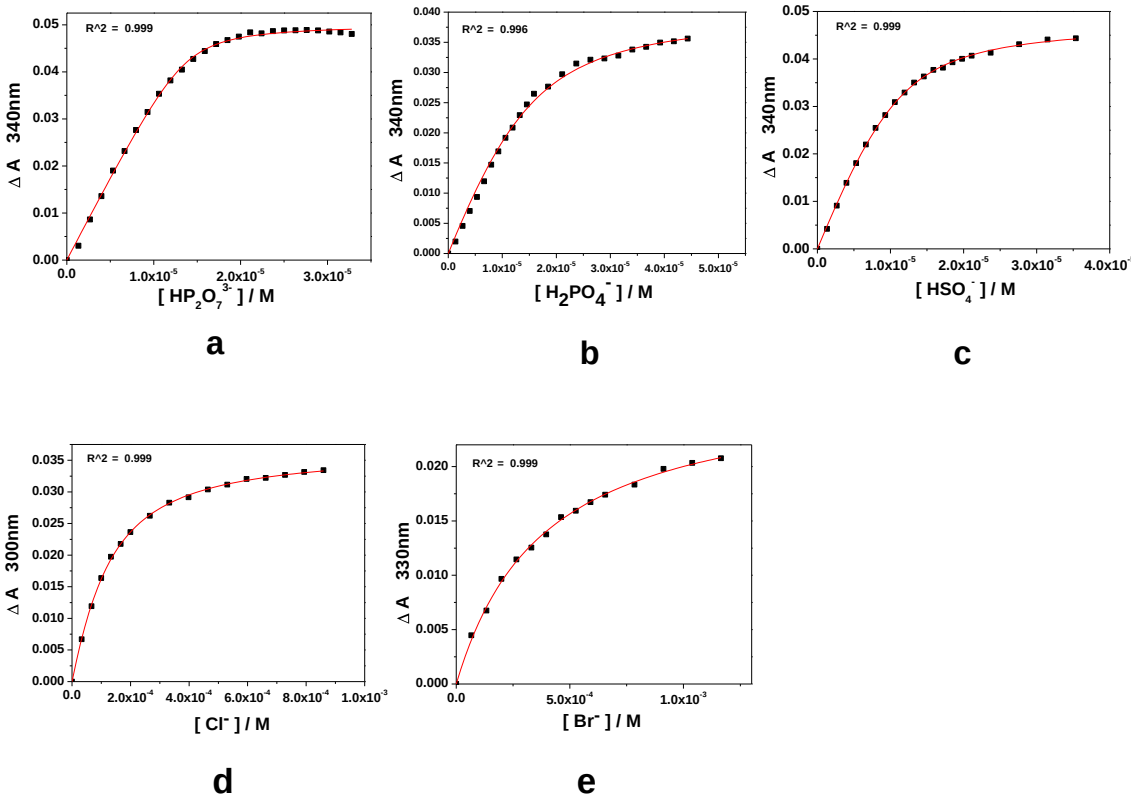

Figure S15: (a) Variations in the absorbance at 340 nm (▪) of a solution of receptor **1** (1.00×10^{-5} M) in $CHCl_3$ as a function of $(TBA)_3HP_2O_7$ concentration (0 ~ 3.0×10^{-5} M) at 300 K. (b) Variations in absorbance (▪) at 340 nm of a solution of receptor **1** (1.00×10^{-5} M) in $CHCl_3$ as a function of $TBAH_2PO_4$ concentration (0 ~ 5.0×10^{-5} M) at 300 K. (c) Variations in absorbance (▪) at 340 nm of a solution of receptor **1** (1.00×10^{-5} M) in $CHCl_3$ as a function of $TBAHSO_4$ concentration (0 ~ 3.0×10^{-5} M) at 300 K. (d) Variations in absorbance (▪) at 300 nm of a solution of receptor **1** (1.00×10^{-5} M) in $CHCl_3$ as a function of TBACl concentration (0 ~ 8.0×10^{-4} M) at 300 K. (e) Variations in absorbance (▪) at 330 nm of a solution of receptor **1** (1.00×10^{-5} M) in $CHCl_3$ as a function of TBABr concentration (0 ~ 1.25×10^{-3} M) at 300 K.

NMR Anion Recognition Study:
Solutions of receptor **1** (5 mM, $CDCl_3$, 300 K) were titrated by adding known quantities of a concentrated solution of various tetrabutylammonium anion salts. The anion solutions used to effect the titration contained the receptors at the same concentration as the receptor solutions into which they were being titrated so as to obviate the need to account for dilution effects during the titrations.

Table S1: Chemical shift changes for selected signals of **1** seen in the presence of 10 equiv. $TBA_3HP_2O_7$, $TBAH_2PO_4$, $TBAHSO_4$, TBACl and TBABr. The changes are relative to what is seen for pure **1**.

	Δδ / ppm					
^{1}H	a	b	c	d	e	f
1·$TBA_3HP_2O_7$	5.094	1.792	1.211	0.277	0.088	-0.296
1·$TBAH_2PO_4$	2.196	2.114	1.664	0.342	0.189	-0.124
1·$TBAHSO_4$	1.265	1.125	0.409	0.299	0.185	-0.111
1·TBACl	3.172	1.072	-0.050	-0.107	0.049	-0.285
1·TBABr	2.102	1.029	-0.068	-0.026	0.075	-0.227

The pyrrole NH hydrogen signal (a), the triazole hydrogen signal (b) and the endocyclic hydrogen atom of the N^1-linked phenyl unit (c) all undergo significant shift when anions are added (Table S1); this is consistent with the proposition put forward in the text, namely that the N-H and C-H are all involved in anion binding.

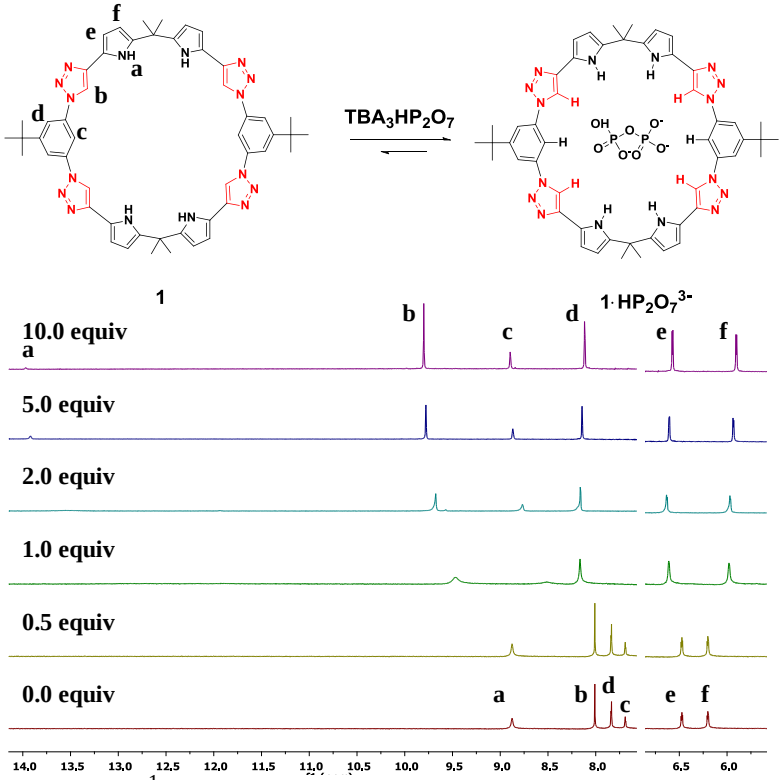

Figure S16. ^{1}H NMR spectrum of macrocycle **1** and 0.5, 1.0, 2.0, 5.0, 10.0 equiv. $TBA_3HP_2O_7$ recorded in $CDCl_3$ at 300 K.

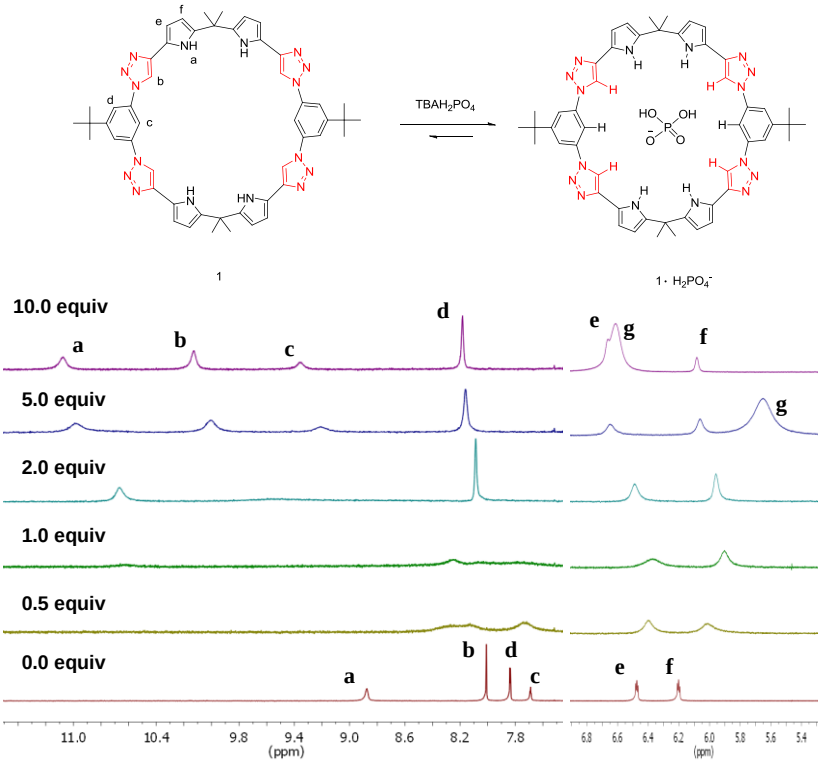

Figure S17. ^{1}H NMR spectrum of macrocycle **1** and 0.5, 1.0, 2.0, 5.0, 10.0 equiv. $TBAH_2PO_4$ recorded in $CDCl_3$ at 300 K. (Peak 'g' is as ascribed to the $H_2PO_4^-$ anion.)

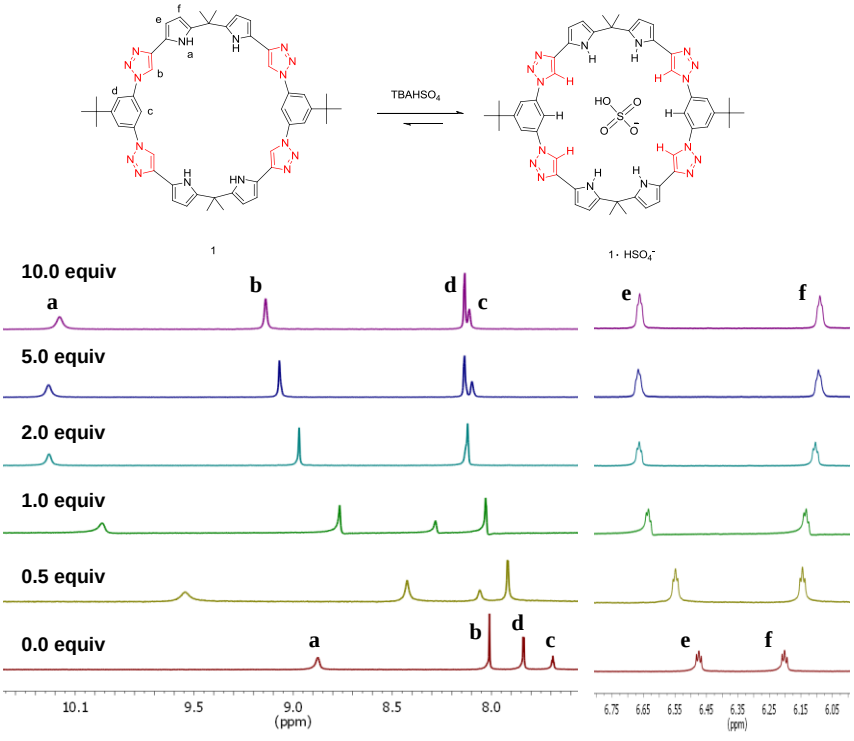

Figure S18. ^{1}H NMR spectrum of macrocycle **1** and 0.5, 1.0, 2.0, 5.0, 10.0 equiv. $TBAHSO_4$ recorded in $CDCl_3$ at 300 K.

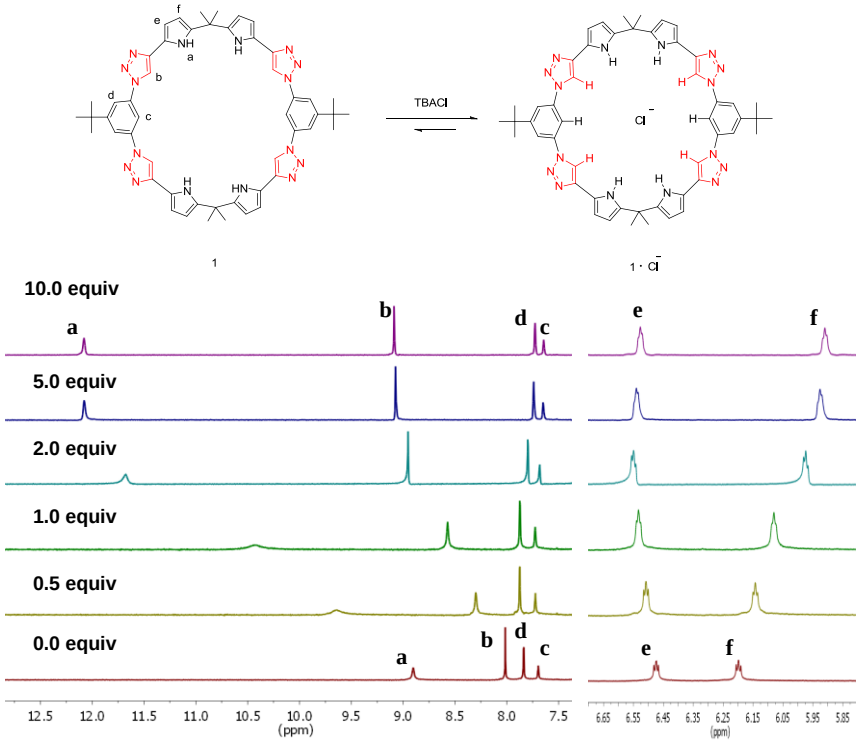

Figure S19. ^{1}H NMR spectrum of macrocycle **1** and 0.5, 1.0, 2.0, 5.0, 10.0 equiv. TBACl recorded in $CDCl_3$ at 300 K.

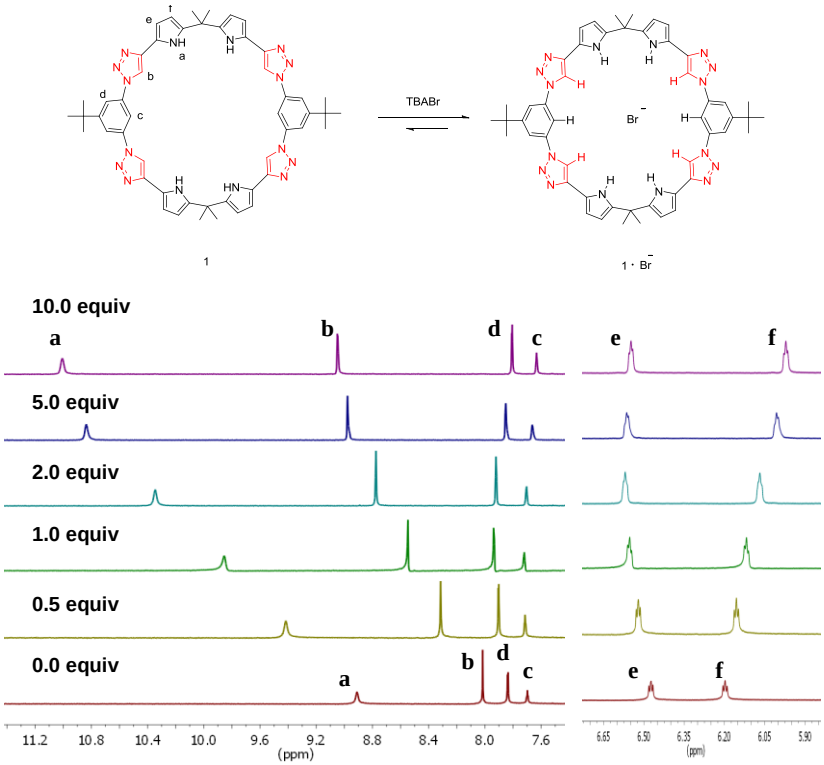

Figure S20. ^{1}H NMR spectrum of macrocycle **1** and 0.5, 1.0, 2.0, 5.0, 10.0 equiv. TBABr recorded in $CDCl_3$ at 300 K

Section S3: Details of High Resolution ESI Mass Spectrometric Study

Table S2. ESI High Resolution Mass Spectra Study for Complexes:

	Host : Guest	Complex	Calculated (m/z)	Found (m/z)
a	1:1	$[(\mathbf{1} \cdot TBA_3HP_2O_7) + TBA]^+$ $C_{114}H_{197}N_{20}P_2O_7$	2020.5143	2020.5171
b	1:1	$[(\mathbf{1} \cdot TBAH_2PO_4) + TBA]^+$ $C_{82}H_{126}N_{18}PO_4$	1457.9941	1457.9942
c	1:1	$[(\mathbf{1} \cdot TBAHSO_4) + TBA]^+$ $C_{82}H_{125}N_{18}SO_4$	1457.9846	1457.9832
d	1:1	$[(\mathbf{1} \cdot TBACl) + TBA]^+$ $C_{82}H_{124}N_{18}Cl$	1395.9939	1395.9977
e	1:1	$[(\mathbf{1} \cdot TBABr) + TBA]^+$ $C_{82}H_{124}N_{18}Br$	1439.9434	1439.9448

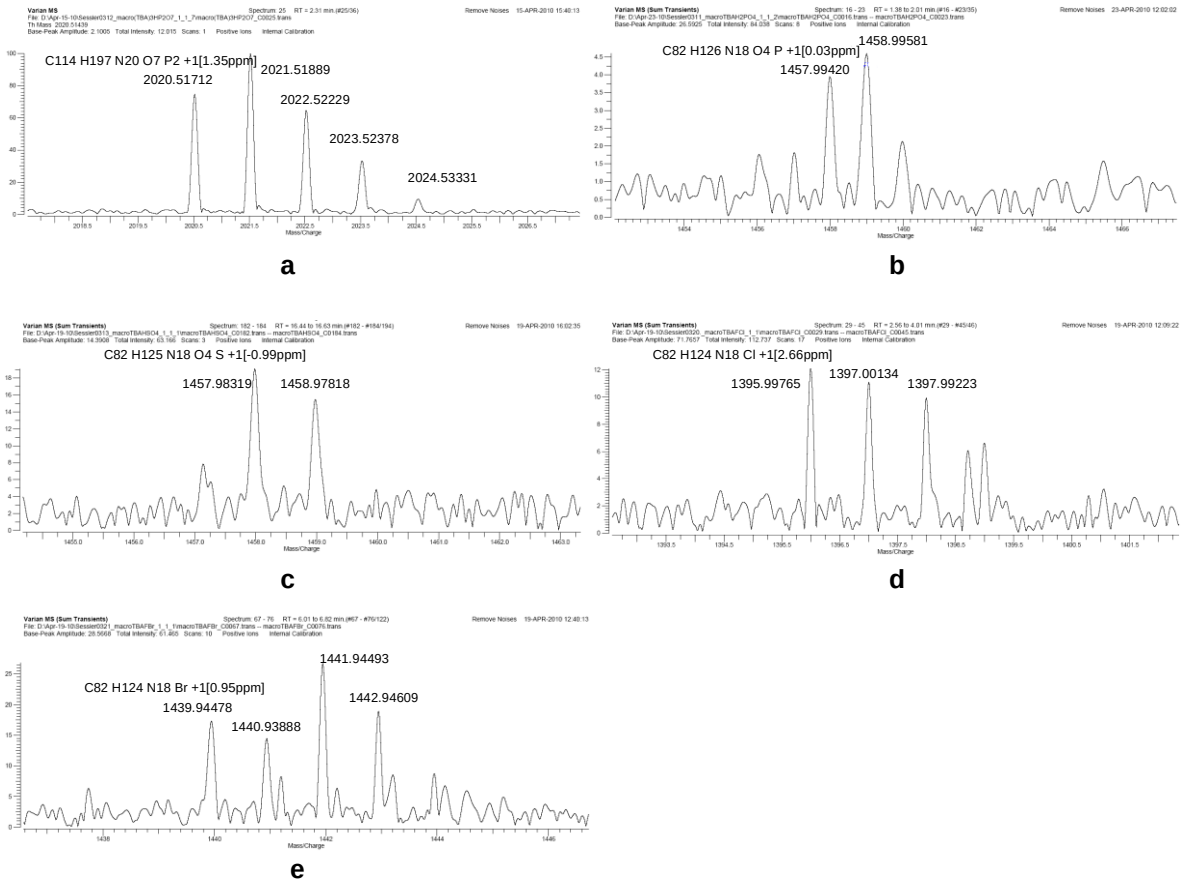

Figure S21: ESI high resolution mass spectrum of samples containing, respectively, 1 molar equiv. of $TBA_3HP_2O_7$ (a), $TBAH_2PO_4$ (b), $TBAHSO_4$ (c), TBACl (d), TBABr (e) and host **1**.

Section S4: Details of Electronic Structure Calculations

Binding energy, ΔE = E(complex) – E(chloride) – E(donor) values were calculated at the MP2/aug-cc-pVDZ level of theory with NWChem.[5] Cartesian coordinates and absolute energies for geometries optimized with NWChem at the MP2/aug-cc-pVDZ level of theory using the frozen core approximation are reported below.

Cl anion

Energy –459.7227644 hartree

Pyrrole

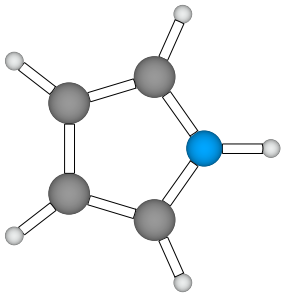

```
Energy -209.5630199 hartree
10
  C    1.131607   -0.714996    0.029633
  C   -0.200928   -1.132996   -0.005264
  C    1.131607    0.714996    0.029633
  C   -0.200928    1.132996   -0.005264
  N   -0.987671    0.000000   -0.025864
  H    2.000305   -1.369995    0.052383
  H   -0.641785   -2.127000   -0.016815
  H    2.000305    1.369995    0.052383
  H   -0.641785    2.127000   -0.016815
  H   -2.000305    0.000000   -0.052383
```

Pyrrole chloride complex

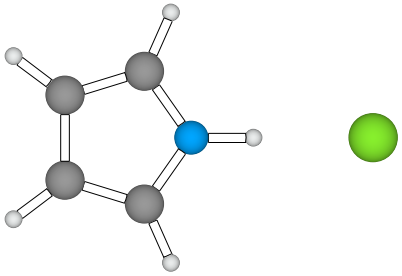

N---Cl = 3.073 Å ; N-H---Cl = 2.020 Å

Energy −669.3216376 hartree

```
11
  C    2.157608   -0.714996   -0.226776
  C    0.819977   -1.121994   -0.086182
  C    2.157608    0.714996   -0.226776
  C    0.819977    1.121994   -0.086182
  N    0.035309    0.000000   -0.003708
  H    3.020859   -1.375000   -0.317505
  H    0.374435   -2.112991   -0.039352
  H    3.020859    1.375000   -0.317505
  H    0.374435    2.112991   -0.039352
  H   -1.011917    0.000000    0.106354
 Cl   -3.020844    0.000000    0.317505
```

Benzene

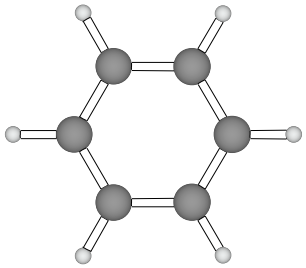

Energy −231.5398383 hartree

```
12
  C   -0.363998    1.359985    0.000000
  C   -1.359985    0.363998    0.000000
  C   -0.995987   -0.995987    0.000000
  C    0.363998   -1.359985    0.000000
  C    1.359985   -0.363998    0.000000
  C    0.995987    0.995987    0.000000
  H   -0.647995    2.416992    0.000000
  H   -2.416992    0.647995    0.000000
  H   -1.768997   -1.768997    0.000000
  H    0.647995   -2.416992    0.000000
  H    2.416992   -0.647995    0.000000
  H    1.768997    1.768997    0.000000
```

Benzene chloride complex

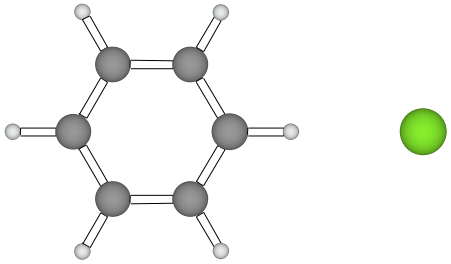

C---Cl = 3.491 Å; C-H---Cl = 2.388 Å

Energy -691.2765323 hartree

```
13
 Cl    3.699539    0.000000    0.291153
  C   -1.901123   -1.217987   -0.149612
  C   -0.496460   -1.212997   -0.039078
  C    0.219315    0.000000    0.017258
  C   -0.496460    1.212997   -0.039078
  C   -1.901123    1.217987   -0.149612
  C   -2.607941    0.000000   -0.205246
  H    1.318909    0.000000    0.103790
  H   -2.447433   -2.168000   -0.192612
  H    0.055832   -2.157990    0.004395
  H    0.055832    2.157990    0.004395
  H   -2.447433    2.168000   -0.192612
  H   -3.699554    0.000000   -0.291153
```

1,2,3-triazole

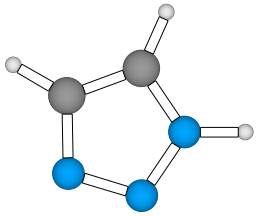

Energy -241.5979766 hartree

```
8
  C   -0.402557    0.546936    0.000000
  C   -0.621628   -0.829620    0.000000
  N    0.956009    0.644669    0.000000
  N    1.561417   -0.566986    0.000000
  N    0.583588   -1.478409    0.000000
  H   -1.060898    1.410828    0.000000
  H   -1.561432   -1.375351    0.000000
  H    1.534958    1.478424    0.000000
```

1,2,3-triazole chloride complex, bound to N-H

(global minimum geometry)

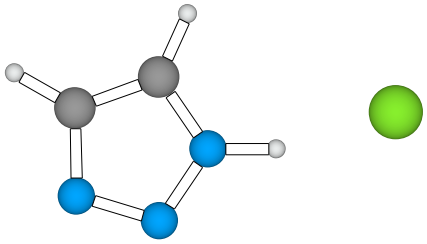

N---Cl = 2.987 Å; N-H---Cl = 1.950 Å

Energy -701.3667612 hartree

9

C	-0.722931	0.623535	0.000000
C	-2.034409	0.142654	0.000000
N	0.041397	-0.496643	0.000000
N	-0.713638	-1.614517	0.000000
N	-2.006256	-1.225784	0.000000
H	-0.277451	1.614517	0.000000
H	-2.974121	0.691391	0.000000
H	1.109436	-0.496643	0.000000
Cl	2.974121	0.072388	0.000000

1,2,3-triazole chloride complex, bound to C-H

(C-H---Cl constrained to 180°)

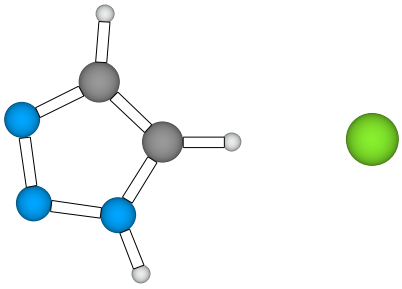

C---Cl = 3.349 Å; C-H---Cl = 2.244 Å

Energy -701.3509268 hartree

9

C	-0.553238	0.031158	0.000000
C	-1.566360	0.991150	0.000000
N	-1.264648	-1.130493	0.000000
N	-2.606537	-0.947678	0.000000
N	-2.795837	0.382050	0.000000
H	0.551865	0.031174	0.000000
H	-1.473282	2.074097	0.000000
H	-0.891617	-2.074097	0.000000
Cl	2.795853	0.070328	0.00000

Section S5: Crystallographic Data (CIF)

Crystals used in this study were in the form of multiply intergrown, colorless needles in the case of macrocycle **1**·$4H_2O$·H_2O, and yellow prisms in the cases of the complex **1**·$TBA_3HP_2O_7$·$3H_2O$. Diffraction grade crystals of macrocycle **1**·$4H_2O$·H_2O were obtained by slow evaporation from solution using a $CHCl_3$ / CH_3OH mixture. Crystals of the complex **1**·$TBA_3HP_2O_7$·$3H_2O$ were obtained by slow evaporation from solution using $CHCl_3$. The data crystals were cut from a cluster of crystals and had the approximate dimensions given in Table S3. The data were collected on a Rigaku Saturn CCD diffractometer using a graphite monochromator with MoKα radiation (λ = 0.71075 Å). The data were collected using ω-scans with a scan range of 1˚ at low temperature shows using an Oxford Cryostream low temperature device (*cf.* Table S3). Data reduction was performed using DENZO-SMN.[6] The structures were solved by direct methods using SIR97[7] and refined by full-matrix least-squares on F^2 with anisotropic displacement parameters for the non-H atoms using SHELXL-97.[8] The hydrogen atoms were calculated in ideal positions with isotropic displacement parameters set to 1.2xUeq of the attached atom (1.5xUeq for methyl hydrogen atoms).

The function, $\Sigma w(|Fo|^2 - |Fc|^2)^2$, was minimized. Definitions used for calculating R(F), $Rw(F^2)$ and the goodness of fit, S, are given below.[9] Neutral atom scattering factors and values used to calculate the linear absorption coefficient are from the International Tables for X-ray Crystallography (1992).[10] All ellipsoid figures were generated using SHELXTL/PC.[11] Tables of positional and thermal parameters, bond lengths and angles, torsion angles, figures and lists of observed and calculated structure factors are located in the cif documents available from the Cambridge Crystallographic Centre *via* quoting ref. numbers 786883 and 786884. These documents also contain details of crystal data, data collection and structure refinement.

Table S3. X-ray crystallographic data comparison of macrocycle **1**·$4H_2O·H_2O$ and complex **1**·$TBA_3HP_2O_7·3H_2O$.

	Macrocycle **1**·$4CH_3OH·H_2O$	Complex **1**·$TBA_3HP_2O_7·3H_2O$
CCDC No.	786884	786883
empirical formula	$C_{54}N_{16}O_5H_{70}$	$C_{98}N_{19}P_2O_{10}H_{167}$
Fw	1021.24	1826.39
crystal size (mm^3)	0.31× 0.13 × 0.02	0.37× 0.11 × 0.02
Crystal system	Monoclinic	Monoclinic
Space group	P2/c	P2(1)/c
a [Å]	18.799(4)	17.507(4)
b [Å]	7.4924(15)	39.237(8)
c [Å]	23.685(5)	24.684(5)
α [deg]	90.00	90.00
β [deg]	125.38(3)	131.52(3)
γ [deg]	90.00	90.00
V / [$Å^3$]	2719.9(9)	12694(4)
d / [g/cm^3]	1.247	0.956
Z	2	4
T [K]	223(2)	113(1)
R1, wR2 $I > 2ó(I)$	0.0929, 0.2083	0.0979, 0.2669
R1, wR2 (all data)	0.1945, 0.2700	0.1368, 0.2973
Quality of fit	0.986	0.973

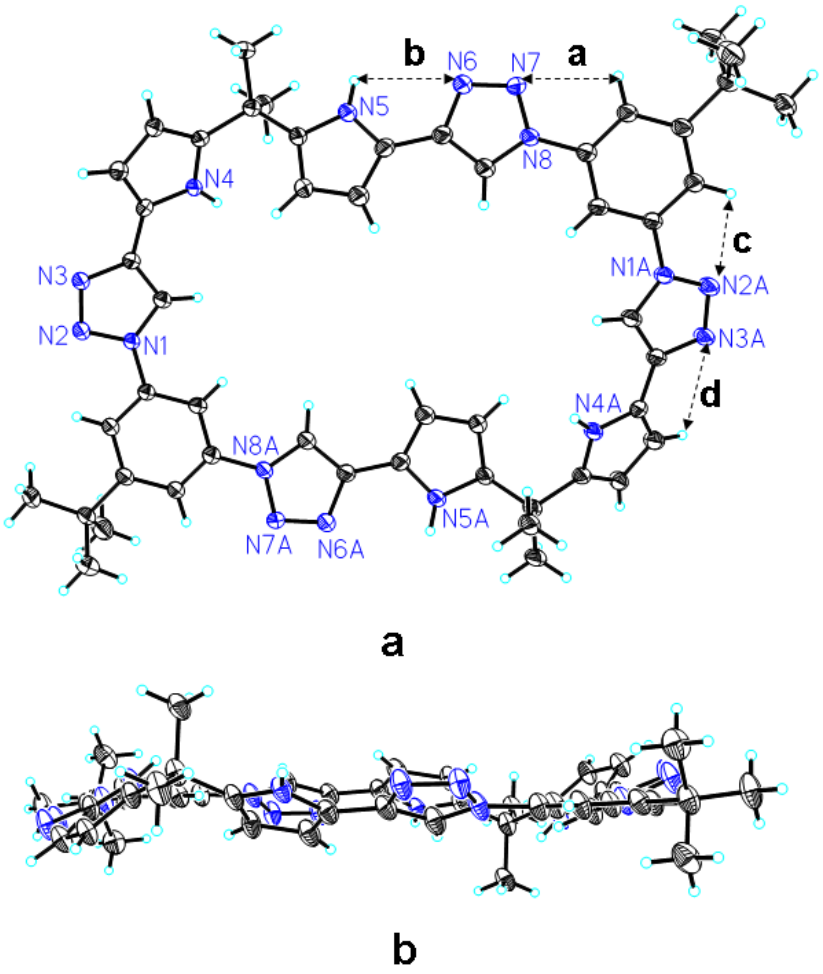

Figure S22: Views of the single crystal X-ray structure of **1**·4CH_3OH·H_2O. All solvent molecules have been omitted for clarity and thermal ellipsoids drawn at the 25% probability level. Symmetry operator (-x, 1-y, -z) generates equivalent atoms marked with "A". **a**, Top view and **b**, side view showing the near planar conformation of **1**. Selected distances [Å]: a = 2.558, b = 2.744, c = 2.601, d = 3.056. This leads us to suggest that intramolecular H-bonding interactions on the exterior of the ring help stabilize the observed planar conformatioin in the solid state; see text proper.

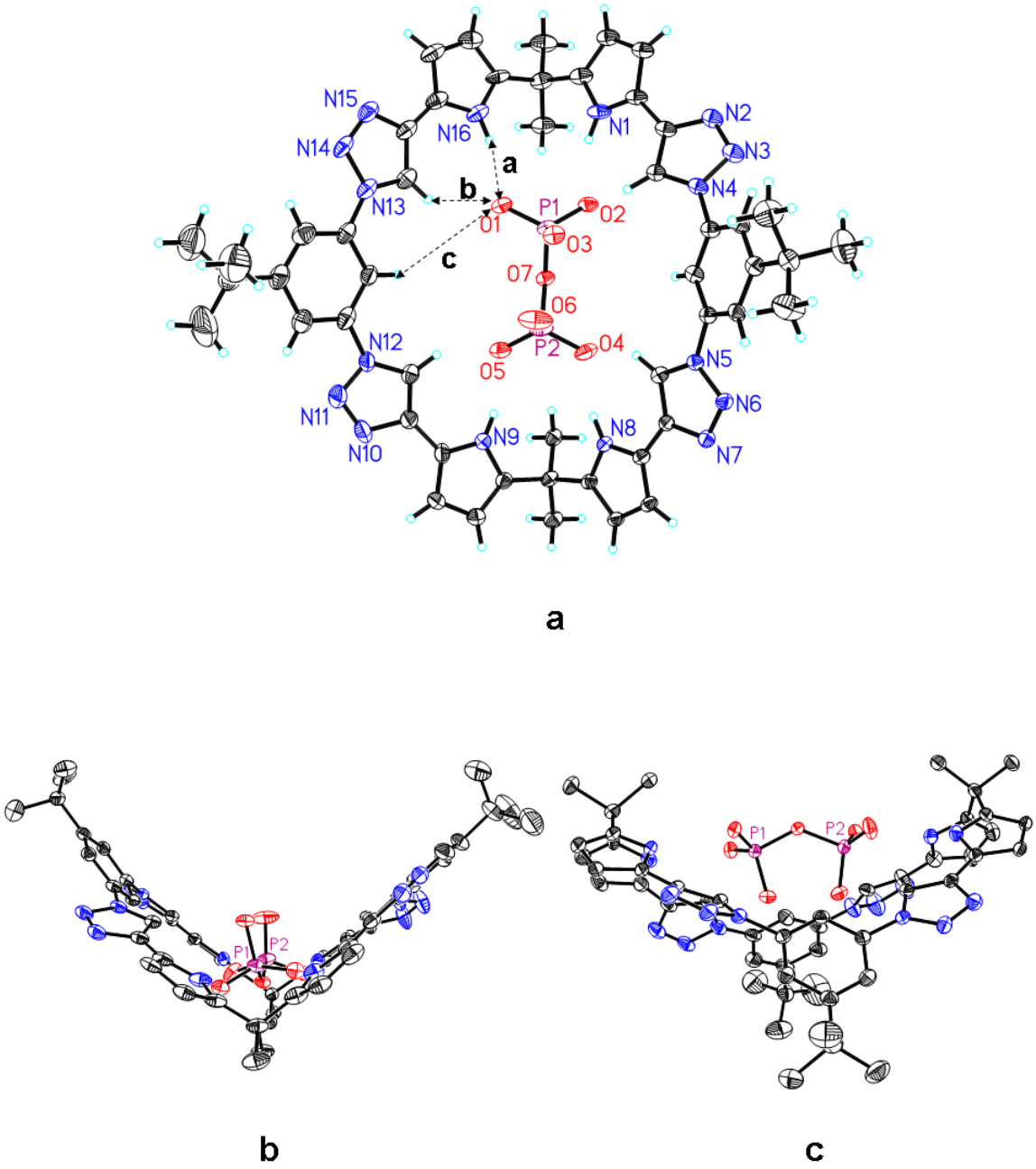

Figure S23: Views of the single crystal X-ray structure of **1**·$TBA_3HP_2O_7$·$3H_2O$. All solvent molecules and TBA cations have been omitted for clarity and thermal ellipsoids drawn at the 25% probability level. **a**, Top view and **b**, **c** side view showing that the pyrophosphate anion is in a space filling representation. Selected distances [Å]: a = 1.905, b = 2.324, c = 3.870. This confirms that pyrrole NH and triazole CH protons are involved in hydrogen bond interactions with pyrophosphate guest; see text proper.

Section S6: References for Supporting Material

(1) Sandström, J. *Dynamic NMR Spectroscopy*; Academic: London, **1982**.

(2) Ōki, M. *Applications of Dynamic NMR Spectroscopy to Organic Chemistry*; WILEY-VCH: Weinheim, **1985**.

(3) Neuhaus, D.; Williamson, M.P. *The Nuclear Overhauser Effect in Structural and Conformational Analysis*; VCH Publishers: Cambridge, U. K., **1989**.

(4) Friebolin, H. *Basic One- and Two-Dimensional NMR Spectroscopy*; WILEY-VCH: Weinheim, **2005**.

(5) Bylaska, E. J.; de Jong, W. A.; Kowalski, K.; Straatsma, T. P.; Valiev, M.; Wang, D.; Apra, E.; Windus, T. L.; Hirata, S.; Hackler, M. T.; Zhao, Y.; Fan, P. –D.; Harrison, R. J.; Dupuis, M.; Smith, D. M. A.; Nieplocha, J.; Tipparaju, V.; Krishnan, M.; Auer, A. A.; Nooijen, M.; Brown, E.; Cisneros, G.; Fann, G. I.; Fruchtl, H.; Garza, J.; Hirao, K.; Kendall, R.; Nichols, J. A.; Tsemekhman, K.; Wolinski, K.; Anchell, J.; Bernholdt, D.; Borowski, P.; Clark, T.; Clerc, D.; Dachsel, H.; Deegan, M.; Dyall, K.; Elwood, D.; Glendening, E.; Gutowski, M.; Hess, A.; Jaffe, J.; Johnson, B.; Ju, J.; Kobayashi, R.; Kutteh, R.; Lin, Z.; Littlefield, R.; Long, X.; Meng, B.; Nakajima, T.; Niu, S.; Pollack, L.; Rosing, M.; Sandrone, G.; Stave, M.; Taylor, H.; Thomas, G.; van Lenthe, J.; Wong, A.; Zhang, Z. *NWChem, A Computational Chemistry Package for Parallel Computers, Version 5.0*, **2006**, Pacific Northwest National Laboratory, Richland, Washington 99352-0999, USA.

(6) DENZO-SMN. (**1997**). Otwinowski, Z.; Minor, W. *Methods in Enzymology*, 276: *Macromolecular Crystallography, Part A*, 307 – 326, Carter, C.W.J.; Simon, M.I.; Sweet, R.M. Editors, Academic Press.

(7) SIR97. (**1999**). A program for crystal structure solution. Altomare, A.; Burla, M. C.; Camalli, M.; Cascarano, G. L.; Giacovazzo, C.; Guagliardi, A.; Moliterni, A.G. G.; Polidori, G.; Spagna, R. *J. Appl. Cryst.* **1999**, *32*, 115-119.

(8) Sheldrick, G. M. *SHELXL*97. *Program for the Refinement of Crystal Structures*; University of Gottingen, Germany, **1994**.

(9) $R_w (F^2) = \{\Sigma w(|Fo|^2 - |Fc|^2)^2/\Sigma w(|Fo|)^4\}^{1/2}$ where w is the weight given each reflection. $R(F) = \Sigma(|Fo| - |Fc|)/ \Sigma|Fo|\}$ for reflections with $Fo > 4(\sigma(Fo))$. $S = [\Sigma w(|Fo|^2 - |Fc|^2)^2/(n - p)]^{1/2}$, where n is the number of reflections and p is the number of refined parameters.

(10) *International Tables for X-ray Crystallography*; Wilson, A. J. C., Ed.; Kluwer Academic Press: Boston, **1992**; Vol. C, Tables 4.2.6.8 and 6.1.1.4.

(11) Sheldrick, G.M. (**1994**). SHELXTL/PC (Version 5.03). Siemens Analytical X-ray Instruments, Inc., Madison, Wisconsin, USA.